

Prediction of scoliosis progression with serial three-dimensional spinal curves and the artificial progression surface technique

Hongfa Wu · Janet L. Ronsky · Farida Cheriet ·
Jessica Küpper · James Harder · Deyi Xue ·
Ronald F. Zernicke

Received: 14 October 2008 / Accepted: 14 June 2010 / Published online: 9 July 2010
© International Federation for Medical and Biological Engineering 2010

Abstract Adolescent idiopathic scoliosis (AIS) progression is clinically monitored by a series of full spinal X-rays. To decrease radiation exposure, an artificial progression surface (APS) is proposed to predict progression. Fifty-six acquisitions (posteroanterior radiographs, 0° and 20°) were obtained from 11 AIS patients ($29.8 \pm 9.6^\circ$ Cobb angle). Three-dimensional curves were constructed through vertebral pedicle centers. Three previous serial spinal curves (6-month intervals) were used to construct an APS with a Non-uniform Rational B-Spline surfacing technique. Future progression was achieved by aligning the curves on the APS using the generalized cross-validation extrapolation technique. With three and four previous serial spinal curves, the prediction accuracies of future progression at the next 6-month interval were $4.1 \pm 3.3^\circ$ for Cobb angles and 3.6 ± 3.5 mm for apex lateral deviations. Apex locations and Cobb regions varied within one vertebral level. The proposed technique shows potential as an accurate three-dimensional prediction method for AIS

progression and could help pediatricians make decisions about treatment. However, it could only be applied once before more radiographic data would be needed.

Keywords Scoliosis · Disease progression · Prediction · Artificial progression surface · Radiography

1 Background

Scoliosis is a three-dimensional (3D) spine and trunk deformity associated with pain, osteoarthritis, and in rare cases death via cardiopulmonary complications [29]. It is routinely monitored in clinic with a series of full spinal X-rays, which expose patients to an effective dose of approximately 130 μ Sv [7]. Other imaging modalities have been explored including magnetic resonance (MR) imaging and computed tomography (CT). CT is capable of more accurately imaging measures such as the apex rotational

H. Wu · J. Küpper · D. Xue
Department of Mechanical and Manufacturing Engineering,
Schulich School of Engineering, University of Calgary,
2500 University Drive NW, Calgary,
AB T2N 1N4, Canada
e-mail: howu@ucalgary.ca

J. Küpper
e-mail: johnsojc@ucalgary.ca

D. Xue
e-mail: dxue@ucalgary.ca

J. L. Ronsky (✉)
Faculty of Kinesiology and Department of Mechanical and
Manufacturing Engineering, Schulich School of Engineering,
University of Calgary, 2500 University Drive NW, Calgary, AB
T2N 1N4, Canada
e-mail: jlronsky@ucalgary.ca

F. Cheriet
Département de génie informatique, École Polytechnique de
Montréal, CHU Sainte-Justine, Centre de Recherche, 3175 Côte-
Ste-Catherine, Montreal, QC H3T 1C5, Canada
e-mail: farida.cheriet@polymtl.ca

J. Harder
Department of Orthopaedic Surgery, Alberta Children's
Hospital, 2888 Shaganappi Trail, Calgary, AB T3B 6A8, Canada
e-mail: jharder@ucalgary.ca

R. F. Zernicke
Faculties of Medicine and Kinesiology and the Department of
Mechanical and Manufacturing Engineering, Schulich School of
Engineering, University of Calgary, 2500 University Drive NW,
Calgary, AB T2N 1N4, Canada
e-mail: rfz@ucalgary.ca

angle [23] but has a much greater radiation dose (e.g., abdominal CT doses 7.3 mSv) [7]. MR imaging allows multiplanar views and no radiation [23], but can also have limited use after surgery when metallic implants are present [35]. Plain radiography continues to be the most common method of assessment.

The pathogenesis of spinal deformity progression is still poorly understood. The prevalence of scoliosis severe enough to require treatment by bracing or surgery (Cobb angle $>20^\circ$) is in the range of 0.1–0.5% of the population [30]. The most common form of scoliosis, adolescent idiopathic scoliosis (AIS), may begin in the preteen years but becomes most prominent during the teenage growth spurt. A primary concern of orthopedic surgeons when managing AIS patients with a minor curvature is identifying whether a curve will progress to severe deformity and require treatment. Accurate identification of curves destined to progress requires a clear understanding of the natural history of idiopathic scoliosis. Since there is currently no reliable way to determine which curves will progress, clinical practice is to monitor all scoliosis patients with a series of full spinal X-rays associated with increased radiation exposure and cancer risk in these adolescents [18]. It is desirable to reduce radiation exposure as much as possible for AIS patients.

Multiple factors contribute to scoliotic curve progression. The incidence of curve progression of 5° (Cobb angle) or more varies according to the criteria of progression for different patient groups with different age, sex, initial Cobb angles, curve pattern, inclusion of patients undergoing treatment, and length of follow-up [9, 11, 12, 26]. After prospectively investigating 1,436 children with untreated idiopathic scoliosis of at least 10° , each followed clinically and roentgenographically for one to four follow-up visits for a mean of 3.2 years [32], only a small percentage of those scoliotic curves progressed (14.7%). Specific factors associated with a higher risk of curve progression included: sex (girls predominantly), curve pattern (right thoracic and double curves in girls, and right lumbar curves in boys), maturity (girls before the onset of menses), age (time of pubertal growth spurt), and curve magnitude ($\geq 30^\circ$). Other reports [8, 21] have also highlighted the factors of remaining growth potential, most rapid adolescent skeletal growth (12 years for girls and 14 years for boys), and Risser sign. The greater the initial curves, the stronger the correlation between spinal growth and curve progression ($r = 0.05\text{--}0.64$) [37]. Factors that increase growth rate, inducing asymmetry, or decrease the inherent stability of the spine may encourage the development and progression of scoliosis [22]. Rotation of the curve is an additional parameter to analyze the risk of progression [31]. However, these studies only qualitatively predicted scoliosis progression, i.e., the percent chance that a scoliosis curve will progress. It is not clear to what extent

these factors can accurately predict the progression of scoliotic curves. The relation between these factors and the extent of curve progression is difficult to quantify.

Yamauchi et al. [36] developed an equation with the following five parameters for predicting scoliosis progression: Cobb angle; rotation of the apical vertebra; deviation of apical vertebra; Risser's expected correction; and maturation index of the iliac apophysis. In this study, an increase of 5° or more during more than 2 years was considered to be progression. Unfortunately, the result for predicting progression was poor, with an accuracy of $\pm 10^\circ$. Mehta [21] was able to predict curve progression using the magnitude of the curve and the rib–vertebra angle difference. However, the study was based on infantile scoliosis and therefore the result is not applicable to juvenile or adolescent scoliosis. Korovessis et al. [14] developed a formula for the prediction of progression of adult idiopathic lumbar scoliosis using the Harrington factor, disc index, and lateral spondylolisthesis of the apical vertebra. Even though the prediction accuracy was good, the developed formula was based on adult scoliosis. Consequently, the equation is not suitable for patients with AIS, as the most common curvature in AIS patients is thoracic curvature rather than lumbar curvature.

These previous studies on predicting scoliosis progression appear to only use data from initial diagnosis for analysis, and final follow-ups as reference for judging whether the curve is progressive or stable. However, the development of scoliosis takes some time and the progression and stabilization of different scoliotic curves may vary. Scoliosis develops in a specific manner and its characteristics can plausibly be observed from serial measurements. The objective of this study was to predict a future progressed 3D spinal curve with the previous successive 3D spinal curves. To implement this study, an initial concept of an artificial progression surface (APS) of scoliosis is proposed. A database of 35 consecutive patients with AIS (29 females and six males, 12.3 ± 2.3 years, range 8.6–17.2 years, Cobb angle $30.2 \pm 12.4^\circ$, range $10.1\text{--}69.9^\circ$ at the first visit) is available in the scoliosis research lab at the University of Calgary, acquired between 1997 and 2002. There were 101 consecutive measurements in total. The average of incremental Cobb angle between two consecutive measurements is 3.49° per 6 months, standard deviation 2.31° per 6 months, maximum 14.95° per 6 months, and minimum 0.88° per 6 months. The concept that spinal deformities of AIS patients change smoothly with time is based on the idea that the spine is a continuous natural system that must progress in a continuous manner. It was hypothesized that the progression of 3D spinal deformity can be predicted by a numerical extrapolation technique, and that a sufficient minimum number of spinal curves will provide clinically relevant predictions.

2 Methods

2.1 Data acquisition

Inclusion criteria were comprised of the following: (1) diagnosis of AIS in patients older than 8 years; (2) no instrumentation/surgery during consecutive measurements; and (3) at least three successive follow-ups in 6-month intervals after the initial visit. Due to abrupt changes of spinal curvatures, patients received surgical treatments were excluded in the current study. However, patients received partial bracing were included. Two standing whole-spinal postero-anterior (PA) radiographs were obtained for all patients at each visit (0° and 20° angled down). In the aforementioned database of 35 AIS patients, subjects with missed sagittal plane spinal curves were excluded in the current study. A total of 11 AIS patients (nine females and two males, 11.4 ± 2.4 years, range 8.6–15.5 years, Cobb angle $29.8 \pm 9.6^\circ$, and range 12.2–55.0° at the first visit) met these criteria. The maximum number of available successive measurements for an individual AIS patient was 10, with 56 consecutive measurements in total. The protocol was approved by the University of Calgary Conjoint Health Research Ethics Board. Informed consent was obtained for all study participants.

2.2 Spine curve

Two X-ray images in the PA 0° and 20° orientation at each data acquisition time point of each patient, as well as known fiducial landmarks, were used to reconstruct the 3D model of the spine and rib cage using the direct linear transformation (DLT) technique [15, 19]. A custom designed patient positioning frame was adopted for consistent data acquisition [27]. Six landmarks per vertebra (superior and inferior bases of both pedicles and endplate centers) were identified on each X-ray film to allow 3D reconstruction of the spine. The accuracy of the 3D reconstruction of the spine was assessed by comparing the reconstructed model with precise measurements made with a coordinate measuring machine on 17 thoracic and lumbar vertebrae (T1–L5) extracted from a normal cadaveric spine specimen. The overall accuracy of the 3D reconstruction for the PA 0° and PA 20° stereopair was 5.6 ± 4.5 mm [1].

The tips of pedicles could be identified more precisely than the center of the end plates on PA radiographs. The vertebral digitization errors were less for pedicles than for end plates. Therefore, the 3D spinal curve was mathematically represented by a line passing through the centers of pedicles, instead of the midpoints of the vertebral body. The spinal curve was best fit with a third-order Fourier-series smoothing function [28]. The Fourier series were of the form:

$$f(x) = A_0 + \sum A_n \cos(nx) + \sum B_n \sin(nx) \tag{1}$$

$$x = (\text{input}) * \pi/L, \quad L = \text{length of curve} \tag{2}$$

where *input* is the deviation of curve, the lateral deviation of pedicles on the coronal plane and the sagittal plane in this study; *f(x)* is the elevation of curve, the elevation of each pedicle in this study. For an order $n = 3$, this gave 7 coefficients describing the curve; the first coefficient was the average value of the function on the domain, and others were amplitudes of *sine* and *cosine* waves of different wavelengths being superimposed.

Prediction accuracies of spinal indices, Cobb levels, apical location, spinal length, computed Cobb angle, and lateral deviation at apex were calculated by comparing the predicted data with the reference (actual) values. Similar to the clinical measure of Cobb angle and apex lateral deviation (*Scoliosis Research Society*), a computed Cobb angle was calculated from the angle between normals to the spine curve at inflectional points, apex location of a primary curve, and apex lateral deviation (the distance of the apical point from the vertical line from L₅). Spinal length was calculated as the length from vertebra T1 to L5 on the coronal plane or in space. The computed Cobb angle was slightly greater (13%) than the clinical Cobb angle, but is known to be highly correlated with it ($r = 0.97$) [33]. The inter- and intra-observer variation of computed Cobb angle has been previously reported as 0.4°–1.8° in the frontal plane [6].

2.3 Artificial progression surface

AIS progresses within a self-sustaining biomechanical cycle involving asymmetrical loading of the spine, alteration of vertebral growth, and development of scoliosis deformities [3, 25]. The pathogenesis of AIS is not clearly defined with respect to the manner in which structural deformities develop or the sequence in which they appear.

Here, it was assumed that scoliosis progressed smoothly with time and, thus, spinal curvatures in different time lags would be closely correlated. The shape of the pelvic girdle of a scoliotic patient is usually normal, and the fifth lumbar vertebra (L5) is not typically deformed. Each spinal curve S_t (t is time order) is composed with seventeen 3D coordinates of pedicle centers of vertebrae (thoracic T1–T12 and lumbar L1–L5) in the space, $S_i = \{(x_{t,1} \ y_{t,1} \ z_{t,1}); \dots; (x_{t,j} \ y_{t,j} \ z_{t,j}); \dots; (x_{t,17} \ y_{t,17} \ z_{t,17})\}$ ($t = 1, \dots, n, j = 1, \dots, 17$), n is the number of serial curves. Figure 1 shows four serial spinal curvatures of an AIS patient.

If consecutive 3D spinal curves were collected and erected from the same location, L5, an APS would be formed to represent the scoliosis spatial deformity (Fig. 2).

Due to measurement and 3D reconstruction errors, consecutive spinal curves would not fit exactly on the

Fig. 1 Schematic demonstration of a time series of vectors composed of four successive spinal curves of consecutive measurements (mm) in 6-month intervals, each represented by a smooth curve passing through pedicle centers (circles) of 17 vertebrae (T1–L5) with a third-order Fourier series function

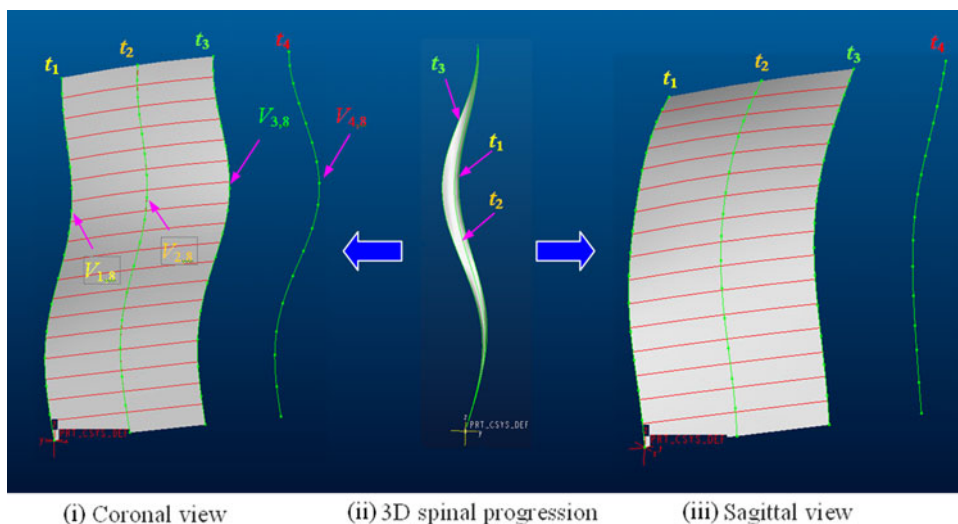
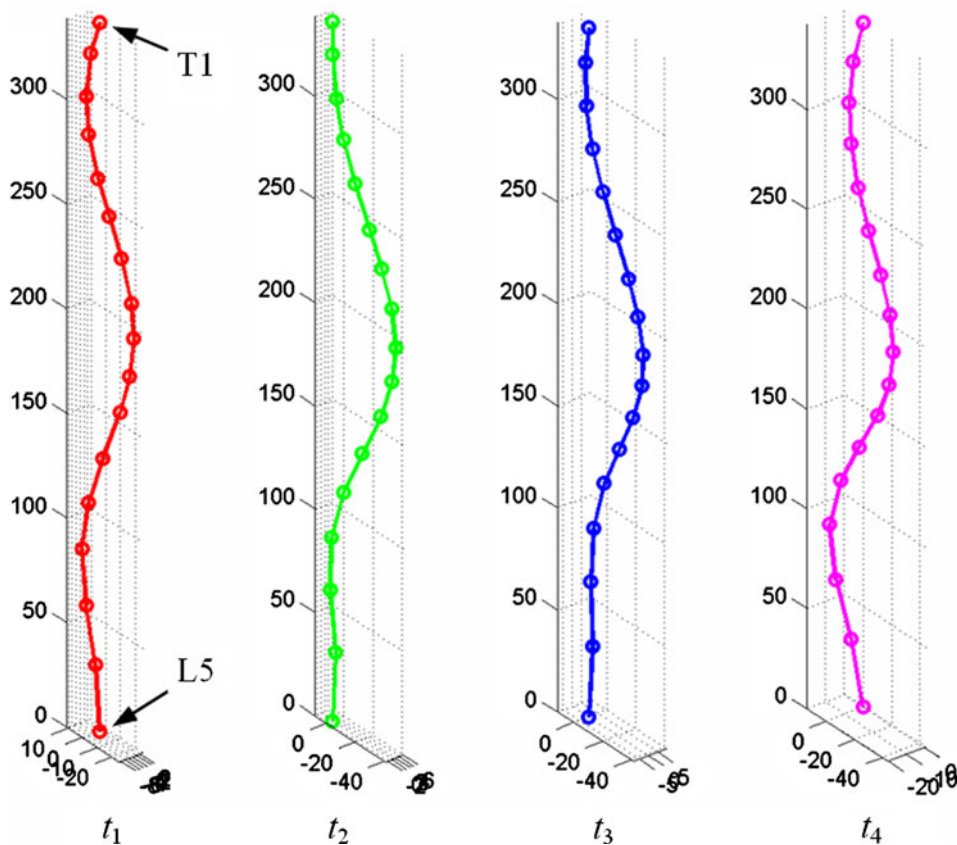


Fig. 2 Schematic demonstration of an APS of scoliosis formed with three successive spinal curves $\{S_{t_1} S_{t_2} S_{t_3}\}$ smoothed by a NURBS surfacing technique. To clearly see the intrinsic features of the APS, the serial spinal curves (ii) were projected on two anatomic planes: coronal (i) and sagittal (iii), and separated by a certain space. Solid points on the spinal curves represent 17 anatomical vertebral centers

(thoracic T1-12 and lumbar L1-5 from the top to the bottom). The vertebral location $V_{4,j}(u,v,w)$ of predicted curve S_{t_4} ($j = 1, \dots, 17$) was individually estimated by corresponding vertebrae $V_{i,j}(u,v,w)$ ($i = 1, 2, 3, j = 1, \dots, 17$) of three fitted curves on the APS $\{Sf_{t_1} Sf_{t_2} Sf_{t_3}\}$ using an extrapolation technique

progression surface. A surface smoothing technique, Non-uniform Rational B-Spline (NURBS) [16], was adopted to smooth the progression surface and to establish

the relation between successive spinal curves and prevent oscillating curve extrapolation. The vertebral locations are control points and the vertices of the

characteristic polyhedron. A parametric NURBS surface was defined as

$$P(u, v) = \sum_{Line=0}^{NLines} \sum_{Vertex=0}^{NVertices} P_{Line,Vertex} B(u)_{Vertex,Order} B(v)_{Line,Order} \tag{3}$$

where $P(u, v)$ is the parametric B-spline approximation, $P_{Line,Vertex}$ is the control polyhedron (i.e., data vertices), and $B(u)$ and $B(v)$ are the normalized basis function values. There are $(NLines + 1) \times (NVertices + 1)$ control vertices in total. $NLines$ was set as 3 for the four serial spinal curve prediction and $NVertices$ as 16 for seventeen vertebrae.

The basis function values were calculated as

$$B_{Vertex,Order}(t) = \left\{ \frac{t - t_{Vertex}}{t_{Vertex+Order-1} - t_{Vertex}} \right\} B_{Vertex,Order-1}(t) + \left\{ \frac{t_{Vertex+Order} - t}{t_{Vertex+Order} - t_{Vertex+1}} \right\} B_{Vertex+1,Order-1}(t) \tag{4}$$

where t represents parameter u and v , $Order$ was set to 4 because a surface of degree 3 in u and v is used most commonly.

The initial conditions for order one were

$$B_{Vertex,1}(t) = \begin{cases} 1 & t_{Vertex} \leq t \leq t_{Vertex+1} \\ 0 & \text{otherwise} \end{cases} \tag{5}$$

Parametric knots were calculated by

$$u_i = \begin{cases} 0, & 0 \leq i < k \\ i - k + 1, & k \leq i \leq n \\ n - k + 2, & n < i \leq n + k \end{cases} \tag{6}$$

$$v_j = \begin{cases} 0, & 0 \leq j < k \\ j - k + 1, & k \leq j \leq m \\ m - k + 2, & m < j \leq m + k \end{cases} \tag{7}$$

where $i = 1, 2, \dots, NLine$ and $j = 1, 2, \dots, NVertices$, $k = Order$ (4 for current study), $n + 1 = NLine + 1$ (number of lines) and $(m + 1) = NVertices + 1$ (number of vertices).

The main features of a NURBS surface are that: (1) it passes through the boundary control curves; (2) it has the local modification property (i.e., the perturbation of the data at one site propagates through limited regions); (3) it has continuous curvatures along control points; and (4) the tangent vectors at the first and last curves are the same as the first and last segments of the control polyhedron.

Two NURBS surfaces were used to incorporate 3D spinal curvatures in the time domain. That is, one NURBS surface was generated with serial spinal curvatures $Sp_t = F_t(x,y)$ in the coronal plane, where t is the number of serial curvatures, x is the vertebra lateral deviation and y is the elevation relative to the fifth lumbar vertebra (L5). The

other NURBS surface was created with serial spinal curvatures $Sp_t = F_t(z,y)$ in the sagittal plane, where z is the vertebra lateral deviation.

Scoliosis progression is not linear with time [11, 14, 15, 28]. A NURBS surface requires at least four curves with at least four vertices. For the case where only three previous curves were available, two additional curves were obtained by interpolating adjacent originals and adding noisy data (normally distributed with mean 0 mm and standard deviation 0.5 mm). For the case of four serial curves, the APS was formed directly from those original curves.

2.4 Prediction of spinal deformity progression

After the smoothing process, all previous $n + 1$ serial original curves $S = \{S_0 \dots S_n\}$ were slightly changed into $Sf = \{Sf_0 \dots Sf_n\}$ to fit onto an APS. The spinal progression S_{n+1} in the next time period was extrapolated as Se_{n+1} from the previous serial fitted curves $\{Sf_0 \dots Sf_n\}$ by

$$\xi_{n+1,j} = \xi_{n,j} + \frac{1}{n-1} \sum_{i=1}^n (\xi_{i+1,j} - \xi_{1,j}) \tag{8}$$

if $sign$ of $(\xi_{n,j} - \xi_{n-1,j}) \neq sign$ of $(\xi_{n-1,j} - \xi_{n-2,j})$, where $\xi_{i,j}$ represents coordinates $(x_{i,j} \ y_{i,j} \ z_{i,j})$ of fitted curves $\{Sf_0 \dots Sf_n\}$ and the estimated curve Se_{n+1} , $i = 0, \dots, n, j = 0, \dots, 16$, otherwise,

$$\xi_{n+1,j} = \xi_{n,j} + \frac{1}{m} \sum_{i=2}^n (\xi_{i+1,j} - \xi_{1,j}) \tag{9}$$

where the optimal number of m was 5.

The prediction accuracies for the main spinal indices on the coronal plane were calculated, such as computed Cobb angle and regions, apex location and lateral deviation, and spinal length, by first quantifying the predicted and actual values of spinal indices. Linear regression values were used to compare between predicted and actual values.

3 Results

The prediction accuracies of different combinations of the number of previous serial spinal curves and the time intervals were investigated. Theoretically, the proposed method can form an APS with any number of previous serial spinal curves. However, to avoid exposing AIS patients to more follow-up radiation risk (i.e., minimize X-ray imaging) while enabling accurate scoliosis progression prediction, the results of three or four previous serial spinal curves only were evaluated. A database of 56 measurements were retrospectively applied for the scoliotic time-series prediction with three previous serial curves $\{S(t_1) \ S(t_2) \ S(t_3)\}$ used to predict for $S(t_4)$ at the next time

interval and $S(t_5)$ at the next second time interval, or four previous serial curves $\{S(t_1) S(t_2) S(t_3) S(t_4)\}$ used to predict for $S(t_5)$ and $S(t_6)$ with 6-month intervals, and three previous curves $\{S(t_1) S(t_2) S(t_3)\}$ with 12-month intervals used to predict for $S(t_4)$ at the next 12 month interval and for $S(t_5)$ at the next 24 month interval. There were not sufficient data of four previous serial curves with 12-month intervals for the prediction of the future curves at 12 month intervals in the database.

Applying the technique of APS of a specific scoliosis formed with previous serial spinal curves successfully predicted the scoliosis future progression in 3D. An example of prediction of scoliosis progression using three previous successive spinal curves is demonstrated in Fig. 3. The spinal curve was represented in the form of $S(x,y,z)$ (Fig. 3iv), where x , y , and z represented coordinates in the PA, mediolateral, and vertical directions, respectively. The 3D curve $S(x,y,z)$ was composed of 2 two-dimensional curves $f(z,y)$ in the coronal plane (Fig. 3i) and $f(z,x)$ in the sagittal plane (Fig. 3ii). A combination of two variables, x and y , forms the third curve $f(x,y)$ in the transverse plane (Fig. 3iii). The results showed that the predicted curve $f(z,y)$ was close to the measured curve, and that the shape of predicted curve $f(z,x)$ in the range of about T1 to T9 was

similar to the measured curve, while the other half of the curve was deviated. The predicted spinal curve $f(x,y)$ had a similar cross-sectional area, but the shapes were different. The prediction accuracy in the coronal plane was higher than in the sagittal and transverse planes because the 3D reconstruction of spine had lower accuracy in the depth (x) compared to lateral and vertical directions (y and z), using the two X-ray images in the PA 0° and PA 20° (angled down) orientations and the DLT technique [1]. Therefore, data presented below for the prediction of scoliosis progression were derived from the coronal plane only, even though the applied technique could predict the future spinal deformity progression in the true 3D, and 3D spinal indices could be further extracted from the 3D curve. Due to normal distribution of the absolute prediction errors, the prediction accuracies were reported with the average absolute values of errors and the standard deviations.

3.1 Serial curves (6-month intervals) to predict progression at next 6 month interval

With 6-month intervals, the prediction accuracies (Table 1) for the future spinal progression $S(t_5)$ at the next 6 month interval using the previous four serial spinal curves $\{S(t_1)$

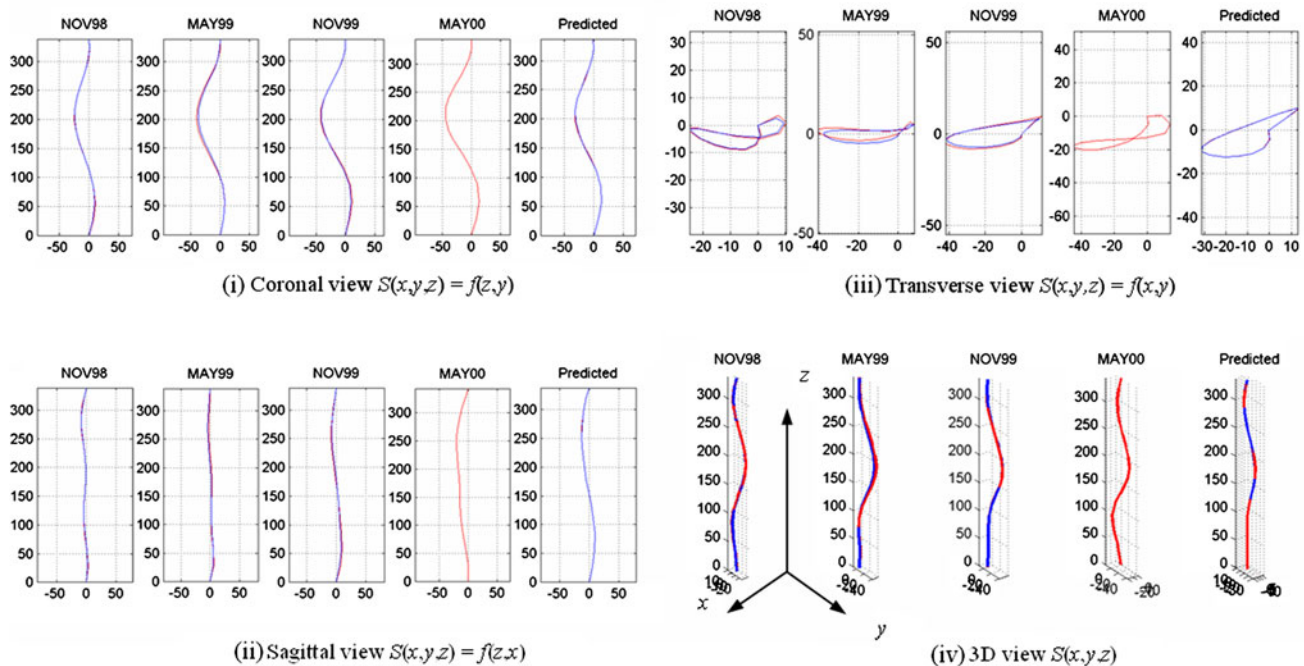


Fig. 3 Schematic demonstration of prediction of future 3D spinal progression S_{i4} of an AIS patient in May 2000 from three previous successive spinal curves S_{i1} , S_{i2} , and S_{i3} in 6-month intervals from November 1998 to November 1999, where S_{ii} was composed of $\{(x_{i,1} y_{i,1} z_{i,1}) \dots (x_{i,17} y_{i,17} z_{i,17})\}$ where $i = 1, \dots, 4$. Results are shown in the **i** coronal, **ii** sagittal, **iii** transverse, and **iv** D views. An APS formed with the three original curves (red line in the first three panels) was smoothed and correlated with the NURBS surfacing technique.

The smoothed (and correlated) curves (blue line) were used to predict the spinal curve S_{i4} (red line in the last panel) with an extrapolation technique, further represented by a smooth curve (blue line in the last panel) with a third-order Fourier series function before the spinal indices (Cobb angle and lateral deviation) were derived. The single curve (red line in the fourth panel) in May 2000 was used as a reference for calculating the prediction accuracy

Table 1 Parameters and variables in predicting algorithm and prediction accuracies

| Groups of data sets | Prediction accuracies (mean ± standard deviation) | | | | | |
|---|---|---|---|---|---|---|
| | 6-month interval | | | 12-month interval | | |
| Method (serial previous data → future one) ^a | $\{S_{t_1} S_{t_2} S_{t_3}\} \rightarrow S_{t_4}$ | $\{S_{t_1} S_{t_2} S_{t_3}\} \rightarrow S_{t_5}$ | $\{S_{t_1} S_{t_2} S_{t_3} S_{t_4}\} \rightarrow S_{t_5}$ | $\{S_{t_1} S_{t_2} S_{t_3}\} \rightarrow S_{t_4}$ | $\{S_{t_1} S_{t_2} S_{t_3}\} \rightarrow S_{t_5}$ | $\{S_{t_1} S_{t_2} S_{t_3} S_{t_4}\} \rightarrow S_{t_5}$ |
| Number of data sets | 36 | 23 | 15 | 15 | N/A | N/A |
| Accuracy of computed Cobb angles (degrees) | 4.7 ± 3.9 | 7.7 ± 7.0 | 3.5 ± 3.0 | 5.0 ± 4.9 | 6.2 ± 8.5 | 7.2 ± 5.4 |
| Regression <i>R</i> -value of computed Cobb angles | 0.95 | 0.73 | 0.95 | 0.68 | 0.4 | 0.7 |
| Accuracy of apex Location (vertebra level) ^b | 0.4 ± 0.7 | 0.5 ± 1.0 | 0.3 ± 0.6 | 0.4 ± 0.5 | 0.1 ± 0.4 | 0.1 ± 0.3 |
| Accuracy of Cobb regions (vertebral level) | 0.2 ± 0.5 | 0.5 ± 1.0 | 0.4 ± 1.0 | 0.6 ± 0.9 | 0.2 ± 0.9 | 0.4 ± 0.5 |
| Accuracy of apex lateral deviation (mm) | 3.9 ± 3.8 | 5.6 ± 5.4 | 3.3 ± 3.3 | 3.2 ± 2.5 | 5.2 ± 8.1 | 4.0 ± 3.9 |
| Regression <i>R</i> -value of apex lateral deviation | 0.90 | 0.68 | 0.82 | 0.79 | 0.36 | 0.81 |
| Accuracy of spinal length (mm) | 9.8 ± 5.8 | 11 ± 7.8 | 9.0 ± 6.2 | 12.7 ± 13.4 | 14.6 ± 12.0 | 10.0 ± 7.7 |

^a Using previous three or four serial spinal curves (abbreviated as $\{S_{t_1} S_{t_2} S_{t_3}\}$ or $\{S_{t_1} S_{t_2} S_{t_3} S_{t_4}\}$) to predict the next one (S_{t_4} or S_{t_5}) at the 6- or 12-month interval. The time intervals are consistent between measurements, either 6- or 12-months

^b The apex is the location of vertebra with the maximum lateral deviation on the curve or the main curve if the spine has multiple curves

$S(t_2) S(t_3) S(t_4)$ were $3.5 \pm 3.0^\circ$ for Cobb angle, 3.3 ± 3.3 mm for apex lateral deviation, and 9.0 ± 6.2 mm for spinal length, while using the previous three serial curves $\{S(t_1) S(t_2) S(t_3)\}$ achieved similarly accurate prediction ($4.7 \pm 3.9^\circ$ for Cobb angle, 3.9 ± 3.8 mm for apex lateral deviation, and 9.8 ± 5.8 mm for spinal length) of future progression $S(t_4)$. The overall prediction accuracies were within an average of $4.1 \pm 3.3^\circ$ and 3.6 ± 3.5 mm, and linear regression *r*-values were 0.95 and 0.88 for Cobb angle and apex lateral deviation, respectively. There are two main reasons that using four serial curves resulted in a more accurate prediction than using the previous three serial curves. First, four serial curves formed a more informative APS than the one with three serial curves and the other two interpolated curves. Second, the NURBS surfacing technique is more suitable for modeling a cubic surface (i.e., with at least four curves) [15]. The prediction accuracies for the apex location and the Cobb regions were in good agreement with each other (a half vertebral level within 95% CI) with both predicting methods. All spinal indices extracted from the predicted spinal curves were excellently correlated with those data from the actual spinal curves (linear regression value $r \geq 0.82$).

3.2 Serial curves (6-month intervals) to predict progression at next 12 month interval

Using the previous three serial curves $\{S(t_1) S(t_2) S(t_3)\}$ with 6 month intervals, the future spinal curves $S(t_5)$ for the next 12 month interval were predicted (Table 1) within accuracies of $7.7 \pm 7.0^\circ$ for Cobb angle, 5.6 ± 5.4 mm for apex lateral deviation, and 11.0 ± 7.8 mm for spinal length. This is less accurate than those of the future progression $S(t_6)$ ($5.0 \pm 4.9^\circ$ for Cobb angle, 3.2 ± 2.5 mm for apex lateral deviation, and 12.7 ± 13.4 mm for spinal length) using the previous four serial curves $\{S(t_1) S(t_2) S(t_3) S(t_4)\}$. The predicted Cobb regions and apex location were within 1.5 and 1.0 vertebra level deviation in both methods. Although the spinal indices from the predicted spinal curves still correlated with the ones from the actual curves well ($r \geq 0.68$), predicting the spinal progression for the next 12 month interval was less accurate than for the next 6 month interval. This reflects a decrease in extrapolation accuracy with an increase in the time interval.

3.3 Serial curves (12-month intervals) to predict progression at next 12 and 24-month interval

With the 12-month intervals, the future spinal progressions (S_{t_4} at the next 12 month interval and S_{t_5} at the next 24 month interval) overall were less accurately predicted with the previous three serial spinal curves; $6.2 \pm 8.5^\circ$ for

Cobb angle, 5.2 ± 8.1 mm for the apex lateral deviation, and 14.6 ± 12.0 mm for the spinal length. The predicted data did not correlate well with the actual data ($r \geq 0.36$). However, the Cobb regions and apex locations were still accurately predicted within 1.0 and 0.5 vertebral level deviation. The results highlight how scoliosis progression changes with time in a complex manner, since spinal deformities are closely linked with spinal muscles, viscera, fat, skin, and rib cage with its incompletely understood mechanisms [5, 34]. The results indicate that progression can be accurately predicted only by previous serial curves with smaller time intervals.

4 Discussion

Scoliosis is a complex 3D spinal deformity and many factors affect scoliosis progression [8, 9, 11, 12, 21, 22, 26, 32, 37]. Previous studies mainly focused on the qualitative prediction of spinal deformity, i.e., the percent chance that a scoliosis curve will progress, by comparing data at the final visit to data at the first visit from spinal images and clinical data. Because different definitions of progression of Cobb angle increase and duration of observation were used in those studies, the outcomes were varied and had limited accuracy. Quantitative prediction techniques of scoliosis progression have been proposed, however, either the outcomes had low accuracy or the proposed methodologies were not suitable for AIS [14, 21, 36]. The present study demonstrated a method to predict a spinal curve based on previous serial spinal curves in 3D. An APS was formed with previous serial curves by applying an NURBS surfacing technique to establish the correlation among those curves and also correct some errors introduced by the measurement system and the 3D reconstruction of spinal curves. Based on the APS, the future spinal curve was predicted based on the spinal curves on the APS with an extrapolation technique.

4.1 Comparison to literature values

The overall prediction accuracies using three and four previous serial spinal curves for the curve at the next immediate future time interval were $4.1 \pm 3.3^\circ$ for the Cobb angle and 3.6 ± 3.5 mm for the apex lateral deviation. The results were very similar to clinical inter/intra-observer variations for measurements of the Cobb angle on radiographs (mean 3.8° of intra-observer, overall standard deviation 2.97°) [4] and 3D spinal reconstruction of the spine (5.6 ± 4.5 mm [1]). Although Korovessis et al. [14] could predict the Cobb angle as accurate as $0.9 \pm 3.8^\circ$ with spinal indices, the method could only be applied for adult idiopathic lumbar scoliosis, not AIS. The deviation of

spinal lengths was predicted within 5% of actual spinal lengths.

4.2 Time series prediction

Time series prediction is an important practical problem with a diverse range of applications from economic and business planning, inventory and production control, weather forecasting, and signal processing and control [2, 10, 24]. Time series are predictable if the behavior of the observed or measured entity is not chaotic or random but associated with a finite number of variables. Most traditional time series models are linear, such as autoregressive and moving averaging. However, there are also many nonlinear time series prediction problems in practical situations, such as prediction of scoliosis progression. The artificial neural network (ANN), a powerful nonlinear tool, has already been used in nonlinear time series modeling in recent years. The most popular neural network model is the feed-forward neural network, in which the back propagation (BP) algorithm is usually used due to its simple architecture yet powerful problem-solving ability. Although vector-valued data can be spread across input neurons as easily as a single number for time series prediction, the database size for training in such cases will be critical to obtain a generalized neural network, mainly depending on the dimension of vectors. For a specific three-layer BP ANN composed of n_i input neurons, m output neurons, and h hidden layer neurons, the minimal number of training samples required is $N_1 = 2 \times (n_i + 1) \times h$. A better sample size would be $2N_1$ [20]. For the current study, each spinal curve had 17 nodes (vertebrae) in 3D and each node had three scalar values. In total there were 51 data values for each spinal curve. If one used three previous spinal curves to predict the next shape, the size of database would be huge and the data acquisition would be impractical to be done expeditiously. In addition, the feed-forward neural network based on the BP algorithm suffers from drawbacks like the multiple local minima problem, the choice of the number of hidden nodes, and a danger of over fitting [20]. In the current study, a new method, APS, was presented to simulate the scoliosis progression and predict the spinal curvature in the next time period by extrapolation.

One important issue often addressed for a time series prediction system is the frequency with which data should be sampled. Clearly, scoliosis progression is nonlinear with time, so using only two consecutive measurements would not allow proper prediction of the scoliosis progression. It has been demonstrated in this study that using a greater number of consecutive curves (e.g., four) can improve the prediction accuracy, but acquiring more X-ray images would mean more radiation exposure. It is a challenge to

obtain high prediction accuracy while using as few radiographs as possible. From the results using different prediction methods, an accurate and clinically significant prediction method that balances these challenges was identified: using three successive spinal curves with 6-month intervals to predict the spinal curve at the next 6-month time point. This result is consistent with the hypothesis that the prediction of spinal curvature would be sufficiently accurate with a minimum number of spinal curves.

4.3 Implications for scoliosis treatment

Three AIS subjects with bracing treatment during the data acquisition period were included in the current study. The detailed treatment information, such as hours per day and days per week, was not recorded for each subject. The serial 3D spinal curves demonstrated that the administration of the bracing treatment changed the course of progression. The predictive ability was poor, i.e., the predicted data were greatly different from the actual data when non-treatment spinal curves were mixed with treatment curves in the serial data sets. There is potential, however, to use this result to evaluate treatment success by comparing the quantified treatment outcome to the modeled untreated progression of spinal deformity.

The sagittal alignment of the thoracic spine is a critical factor when a scoliotic patient is being considered for spinal surgery [17]. Statistically, the mean normal sagittal thoracic alignment from the fifth to the twelfth thoracic vertebra is 30° within a range of $+10^\circ$ to $+40^\circ$. The hypokyphotic sagittal thorax has a curve of less than 10° , while a sagittal thoracic curve of more than 40° is called hyperkyphosis. The technique presented here can predict 3D spinal curves, including the curves of the thoracic spine in the sagittal plane, although the prediction accuracy must be refined to obtain substantial improvements in accuracy over other techniques (e.g., advanced 3D reconstruction DLT technique for photographic images with bundle adjustment).

4.4 Strengths and limitations

The proposed technique of the APS combined can individually predict the scoliosis progression of spinal curve in 3D, as long as sufficient successive measurements are available for a specific patient. No database and full representation of spinal progression patterns were required for computation and improvement of prediction accuracy, while artificial intelligent techniques (e.g., adaptive neuro-fuzzy inference system (ANFIS) and ANN) do require a large database in which similar numbers of members are distributed in all progression patterns. Otherwise, the

trained ANFIS and ANN would not be sufficiently general to predict the scoliosis progression in all cases. Furthermore, ANN and ANFIS could theoretically be used for prediction on any dimensional data. However, this would require a huge database, which is less practical.

A drawback of the technique presented in this study was that the accuracy of the 3D reconstruction of the spine affects the prediction accuracy of 3D spinal curve. Even though, the ANFIS and ANN techniques can remove some errors from the learning process, a more accurate and convenient method of 3D reconstruction of spine is strongly desirable, such as a self-calibration algorithm and a weak-perspective method developed by Kadoury et al. [12]. In addition, the database used in the current study came from a limited number of patients. The presented 3D spatial prediction method with APS for the AIS patients needs to be further validated with a large number of AIS patients. This process is the focus of the current study.

The number of patients involved in the present study was limited (11 patients). Some patients that received partial bracing were included. The effects of bracing, growth spurt, and age versus degree of curve on the prediction accuracy need to be further addressed after more AIS patient data become available. Due to the limited number of recruited AIS patients, the prediction method with APS is still not perfectly defined. It needs to be improved after more AIS patient data becomes available.

In future work, this project aims to quantitatively predict scoliosis progression with limited spinal images; for instance, the spinal image at the first clinic visit only. The correlation between external torso surface changes and internal spinal deformities at individual times will be closely investigated in future studies. As a long term goal, the aim is to quantitatively predict scoliosis progression using primarily torso surface images based on a minimally invasive approach that drastically reduces the number of spinal images required.

4.5 Clinical implications

This study introduced a new concept of an APS formed with previous serial spinal curves, which can correlate the historical spinal deformities for individual AIS patients. The proposed technique provides a promising approach for predicting individual scoliosis progression in 3D with previous serial 3D spinal curves. An accurate and clinically significant prediction method was demonstrated based on three successive spinal curves with 6-month intervals to predict the spinal curve at the next 6-month interval. The prediction accuracy was at least twice as accurate as a typical clinical measurement. This method has the potential benefit of reducing the X-ray dose by half at steady state. After the first 3–4 examinations at a 6 months sampling

rate, the interval between exposures could be lengthened to 12 months. The missed 6 month exposure measurement would then be substituted with the predicted Cobb angle. The long term predictive ability of this technique could be improved by conducting an analysis on a statistically significant number of patients. Improved prediction of scoliosis progression may prove to be important for clinical decision making for monitoring, bracing and surgical treatments and could potentially help to decrease hazardous X-ray exposure levels.

In this study, an APS with a Non-uniform Rational B-Spline surfacing technique is proposed to predict Scoliotic curve progression. The proposed technique shows potential as an accurate three-dimensional prediction method for AIS progression that could reduce radiation exposure, and help pediatricians make decisions about treatment.

Acknowledgments The authors would like to gratefully acknowledge the financial support from Canadian Institutes of Health Research (CIHR), Alberta Children's Hospital Foundation, Fraternal Order of Eagles (Alberta & Saskatchewan), Lew Reed Spinal Cord Injury Foundation, Alberta Ingenuity Fund (AIF), and the Natural Sciences and Engineering Research Council of Canada (NSERC).

References

- Aubin CE, Dansereau J, Parent F et al (1997) Morphometric evaluations of personalised 3d reconstructions and geometric models of the human spine. *Med Biol Eng Comput* 35:611–618
- Bengio S, Fessant F, and Collobert D (1995) A connectionist system for medium-term horizon time series prediction. In: Proceedings of the international workshop on applied neural networks to telecommunications
- Burwell RG, Cole AA, Cook TA et al (1992) Pathogenesis of idiopathic scoliosis. The Nottingham concept. *Acta Orthop Belg* 58(Suppl 1):33–58
- Carman DL, Browne RH, Birch JG (1990) Measurement of scoliosis and kyphosis radiographs. Intraobserver and interobserver variation. *J Bone Joint Surg Am* 72:328–333
- Closkey RF, Schultz AB (1993) Rib cage deformities in scoliosis: spine morphology, rib cage stiffness, and tomography imaging. *J Orthop Res* 11:730–737
- Delorme S, Petit Y, de Guise JA et al (2003) Assessment of the 3-d reconstruction and high-resolution geometrical modeling of the human skeletal trunk from 2-d radiographic images. *IEEE Trans Biomed Eng* 50:989–998
- Don S (2004) Radiosensitivity of children: potential for overexposure in CR and DR and magnitude of doses in ordinary radiographic examinations. *Pediatr Radiol* 34(Suppl 3):S167–S172
- Duval-Beaupere G (1971) Pathogenic relationship between scoliosis and growth. Churchill Livingstone, Edinburgh
- Duval-Beaupere G (1992) Rib hump and supine angle as prognostic factors for mild scoliosis. *Spine* 17:103–107
- Edwards T, Tansley SW, Davey N et al (1997) Traffic trends analysis using neural networks. *Proc Int Workshop Appl Neural Netw Telecom* 3:157–164
- Goldberg CJ, Dowling FE, Hall JE et al (1993) A statistical comparison between natural history of idiopathic scoliosis and brace treatment in skeletally immature adolescent girls. *Spine* 18:902–908
- Kadoury S, Cheriet F, Laporte C, Labelle H (2007) A versatile 3D reconstruction system of the spine and pelvis for clinical assessment of spinal deformities. *Med Bio Eng Comput* 45: 591–602
- Karol LA, Johnston CE 2nd, Browne RH et al (1993) Progression of the curve in boys who have idiopathic scoliosis. *J Bone Joint Surg Am* 75:1804–1810
- Korovessis P, Piperos G, Sidiropoulos P et al (1994) Adult idiopathic lumbar scoliosis. A formula for prediction of progression and review of the literature. *Spine* 19:1926–1932
- Labelle H, Dansereau J, Bellefleur C et al (1995) Variability of geometric measurements from three-dimensional reconstructions of scoliotic spines and rib cages. *Eur Spine J* 4:88–94
- Lee K (1999) Principles of cad/cam/cae systems. Prentice Hall, New York
- Lenke LG, Betz RR, Harms J et al (2001) Adolescent idiopathic scoliosis: a new classification to determine extent of spinal arthrodesis. *J Bone Joint Surg Am* 83-A:1169–1181
- Levy AR, Goldberg MS, Mayo NE et al (1996) Reducing the lifetime risk of cancer from spinal radiographs among people with adolescent idiopathic scoliosis. *Spine* 21:1540–1547
- Marzan GT (1976) Rational design for close range photogrammetry. Ph.D., University of Illinois at Urbana-Champaign, Urbana, IL
- Masters T (1993) Practical neural network recipes in c++. Academic Press, California
- Mehta MH (1972) The rib-vertebra angle in the early diagnosis between resolving and progressive infantile scoliosis. *J Bone Joint Surg Br* 54:230–243
- Murray DW, Bulstrode CJ (1996) The development of adolescent idiopathic scoliosis. *Eur Spine J* 5:251–257
- Oestreich AE, Young LW, Young Poussaint T (1998) Scoliosis circa 2000: radiologic imaging perspective I. Diagnosis and pretreatment evaluation. *Skeletal Radiol* 27:591–605
- Patterson DW, Chan KH, and Tan CM (1993) Time series forecasting with neural nets: A comparative study. In: Proceedings of the international conference on neural network applications to signal processing, Singapore
- Perdriolle R, Becchetti S, Vidal J et al (1993) Mechanical process and growth cartilages. Essential factors in the progression of scoliosis. *Spine* 18:343–349
- Peterson LE, Nachemson AL (1995) Prediction of progression of the curve in girls who have adolescent idiopathic scoliosis of moderate severity. Logistic regression analysis based on data from the brace study of the scoliosis research society. *J Bone Joint Surg Am* 77:823–827
- Poncet P, Delorme S, Ronsky JL, Dansereau J, Clynch G, Harder J, Dewar RD, Labelle H, Gu PH, Zernicke RF (2000) Reconstruction of laser-scanned 3D torso topography and stereoradiographical spine and rib-cage geometry in scoliosis. *Comput Methods Biomech Biomed Eng* 4:59–75
- Poncet P, Dansereau J, Labelle H (2001) Geometric torsion in idiopathic scoliosis: three-dimensional analysis and proposal for a new classification. *Spine* 26:2235–2243
- Pope MH, Stokes IA, Moreland M (1984) The biomechanics of scoliosis. *Crit Rev Biomed Eng* 11:157–188
- Reamy BV, Slakey JB (2001) Adolescent idiopathic scoliosis: review and current concepts. *Am Fam Physician* 64:111–116
- Samuelsson L, Norén L (1997) Trunk rotation in scoliosis. The influence of curve type and direction in 150 children. *Acta Orthop Scand* 68(3):273–276
- Soucacos PN, Zacharis K, Gelalis J et al (1998) Assessment of curve progression in idiopathic scoliosis. *Eur Spine J* 7:270–277

33. Stokes IA, Shuma-Hartwick D, Moreland MS (1988) Spine and back-shape changes in scoliosis. *Acta Orthop Scand* 59:128–133
34. Stokes IA, Dansereau J, Moreland MS (1989) Rib cage asymmetry in idiopathic scoliosis. *J Orthop Res* 7:599–606
35. Wright N (2000) Imaging in scoliosis. *Arch Dis Child* 82:38–40
36. Yamauchi Y, Yamaguchi T, Asaka Y (1988) Prediction of curve progression in idiopathic scoliosis based on initial roentgenograms. A proposal of an equation. *Spine* 13:1258–1261
37. Ylikoski M (1993) Spinal growth and progression of adolescent idiopathic scoliosis. *Eur Spine J* 1:236–239